DOI: 10.1002/ejic.200700366

A Basket-Like $[Sr\subset P_6Mo^{V}_4Mo^{VI}_{14}O_{73}]^{10-}$ Polyoxoanion Modified with $\{Cu(phen)(H_2O)_x\}$ (x = 1–3) Fragments: Synthesis, Structure, Magnetic, and Electrochemical Properties

Kai Yu,[a] Yang-Guang Li,*[b] Bai-Bin Zhou,*[a] Zhan-Hua Su,[a] Zhi-Feng Zhao,[a] and Yu-Nan Zhang[a]

Keywords: Polyoxometalate / Organic–inorganic hybrid / Basket-like / Electrocatalysis

Hydrothermal reaction of a mixture of $Na_2MoO_4{\cdot}2H_2O$, H_3PO_4, $CuCl_2{\cdot}2H_2O$, *o*-phenanthroline, and $SrCl_2$ in water leads to the isolation of a basket-like mixed-valent polymolybdophosphate hybrid compound, $[Cu(phen)(H_2O)_3][\{Cu(phen)(H_2O)_2\}\{Cu(phen)(H_2O)\}_3\{Sr\subset P_6Mo_4{}^{V}Mo_{14}{}^{VI}O_{73}\}]{\cdot}3H_2O$ **1**, which crystallizes in the space group $P\bar{1}$ with a = 13.778(3) Å, b = 19.267(4) Å, c = 24.168(5) Å, α = 110.64(3)°, β = 90.31(3)°, γ = 110.02(3)°, V = 5582.8(2) Å^3, Z = 2. Single-crystal X-ray diffraction analysis shows that the four-electron-reduced basket-like polyoxoanion $[Sr\subset P_6Mo_4{}^{V}Mo_{14}{}^{VI}O_{73}]^{10-}$ contains a new tetravacant γ-Dawson-type unit and a "handle"-shaped $\{P_4Mo_4\}$ segment, which are highly modified with $\{Cu(phen)(H_2O)_x\}$ (x = 1–3) fragments. Electrochemical analysis shows that **1**-modified carbon paste electrode (CPE) displays good electrocatalytic activity to reduce hydrogen peroxide.

Introduction

Polyoxometalate (POM)-based organic–inorganic hybrid compounds have attracted great interest in recent years owing to their extensive theoretical and practical applications in catalysis, molecular adsorption, medicine, electroconductivity, magnetism, and photochemistry.[1–7] A current research interest in this field is modification of the surface of POMs with various organic and/or transition-metal complex moieties.[1–10] These kinds of modified POM derivatives can be regarded as an ideal molecular model for determination of the mechanisms of oxide-supported catalysts.[1] Furthermore, such kinds of compounds can be molecularly fine-tuned and provide potentially new types of catalyst systems as well as interesting functional materials with optical, electronic, and magnetic properties.[1b,1c] During the preparation, two strategies have been exploited to increase the surface charge density and activate the surface oxygen atoms of heteropolyoxoanions:[1] (1) reduce the metal centers from a high oxidation state to a low oxidation state, for example, from Mo^{VI} to Mo^{V}, by introducing strong reducing reagents or (2) replace high-valence metal centers with lower-valence ones, for instance, from Mo^{VI} to V^{IV} or TM^{2+} (TM = transition metal). However, the highly reduced polyoxoanions are usually unstable and inclined to be oxidized in ambient atmosphere. Thus, the hydrothermal technique has been extensively employed and proved to be an efficient way to obtain metastable POMs modified by various organic and/or metal–organic fragments.[2] According to the above-mentioned strategies, a series of hybrid compounds based on Keggin- and Dawson-type heteropolytungstates have been prepared, such as $[\{Ni(bpy)_2(H_2O)\}(PW_{12}O_{40})]^{3-}$,[9a] $[\{Ag(bpy)\}_2\{Ag_2(bpy)_3\}_2(PW_9V_3O_{40})]$,[9b] $[\{Cu(bpy)_2\}(SeW_{12}O_{40})]^{3-}$,[9c] $[\{Cu(PPD)_2\}(As_2W_{18}O_{60})]$,[9d] and $[\{Zn(phen)_2\}\{Zn(phen)_2(H_2O)\}(P_2W_{18}O_{62})]$.[9e] In contrast, most modified polyoxomolybdate composite compounds in earlier research, especially in the work of Zubieta,[2a] concentrated on isopolyoxometalate-supported transition-metal complexes. When PO_4^{3-} was introduced into the $\{MoO_x/TM/L\}$ (TM = transition metal, L = organic ligand) system, a series of reduced polymolybdophosphates decorated with metal–organic units were synthesized.[2b,2c,10–12] It is interesting that most of these hybrid compounds are based on inorganic $\{PMo_{12-x}TM_xO_{40}\}$,[10] $\{P_4Mo_6O_{31}\}$,[11] and $\{P_2Mo_5O_{23}\}$[12] building blocks. More recently, three unusual large clusters, $[P_6Mo_{18}O_{73}]^{11-}$,[13] $[H_{14}(Mo_{16}O_{32})Co_{16}(PO_4)_{24}(H_2O)_{20}]^{10-}$,[14] and $[Na_4(H_2O)_6\{(Mo_2O_4)_{10}(P_2O_7)_{10}(OAc)_8(H_2O)_4\}]^{24-}$[15] have been reported. However, no organic or metal–organic complexes have been successfully coordinated to these highly reduced polymolybdophosphate clusters so far, the reason for which may be that the large size of these POMs decreases the elec-

[a] Academy of Physics and Chemistry, Harbin Normal University, Harbin 150080, P. R. China
E-mail: zhou_bai_bin@sina.com
[b] Key Laboratory of Polyoxometalate Science of Ministry of Education, Faculty of Chemistry, Northeast Normal University,
Changchun, Jilin, 130024, P. R. China
E-mail: liyg658@nenu.edu.cn
Supporting information for this article is available on the WWW under http://www.eurjic.org or from the author.

tron density of the surface or the coordination ability of the surface oxygen atoms. During our continuing research on modified-POM hybrid compounds in the $\{MoO_x/P/TM/L\}$ system, we are interested in employing metal–organic units to decorate high-nuclear clusters in order to get new hybrid materials to explore their fascinating magnetic and electrochemical properties. In this paper, we report the hydrothermal synthesis and crystal structure of a basket-like four-electron reduced polymolybdophosphate hybrid compound, $[Cu(phen)(H_2O)_3][\{Cu(phen)(H_2O)_2\}\{Cu(phen)(H_2O)\}_3\{Sr\subset P_6Mo_4{}^{V}Mo_{14}{}^{VI}O_{73}\}]\cdot 3H_2O$ **1**. In the crystal structure of **1**, the basket-like polyoxoanion contains a new tetravacant γ-Dawson-type unit and a "handle"-shaped $\{P_4Mo_4\}$ segment, which are decorated by four $\{Cu(phen)(H_2O)_x\}$ (x = 1–3) fragments. The magnetic, electrochemical, and electrocatalytic properties of compound **1** were also investigated.

Results and Discussion

Syntheses

The successful isolation of compound **1** relies on the employment of a hydrothermal technique. Hydrothermal synthesis has recently been proved to be a particularly effective method for the preparation of new organic–inorganic hybrid materials.[2,6–15] Exploitation of hydrothermal conditions provides a paradigm shifting from the thermodynamics to the kinetics. Under such conditions, equilibrium phases are replaced by structurally more complex metastable phases.[2,16] In the hydrothermal environment, the reduced viscosity of water results in enhanced rates of solvent extraction from solids and crystal growth from solution.[2] Further, as different solubility problems can be minimized, a variety of organic and inorganic precursors can be introduced.[2] Meanwhile, hydrothermal synthesis is still a relatively complex process because many factors can influence the outcome of a reaction, such as the type of initial reactants, starting concentrations, pH value, reaction time, and temperature.[2,16] However, numerous successful experimental results from these so-called "black-box" reactions could suggest some preliminary synthetic experiences, which might be helpful for the future synthetic route.

During our exploration of the hybrid polymolybdophosphates modified with various organic and/or metal–organic complex fragments, abbreviated as the $\{MoO_x/P/TM/L\}$ (TM = transition metal; L = N donor organic ligand) system, a series of new composite compounds have been hydrothermally synthesized as shown in Table 1.[10–12] It is noteworthy that almost all the compounds can be separated into three groups on the basis of their POM building blocks, that is, $\{PMo_{12-x}TM_xO_{40}\}$, $\{P_4Mo_6O_{31}\}$, and $\{P_2Mo_5O_{23}\}$ units (see Figure 1). During the preparations, although various molar ratios of $Na_2MoO_4/H_3PO_4/TM^{2+}$/L were used, the initial pH value and the reaction temperature seem to be vital for a successful reaction. As shown in Figure 1, the $\{P_2Mo_5\}$-based composite compounds are generally isolated at 160 °C, whereas most $\{P_4Mo_6\}$-based compounds could be prepared above 180 °C. Further, both $\{P_2Mo_5\}$- and $\{P_4Mo_6\}$-based compounds can be synthesized in a wide range of pH values, whereas the $\{PMo_{12-x}TM_xO_{40}\}$-based compounds can only be prepared in a very narrow pH range of ca. 3.5–4.

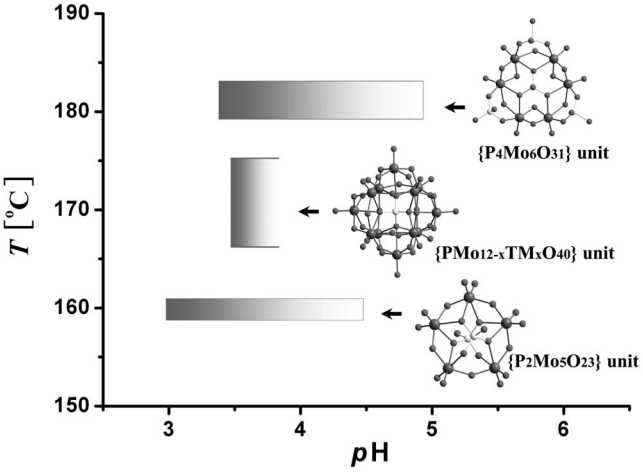

Figure 1. Illustration of possible synthetic products in the $\{MoO_x/P/TM/L\}$ system based on three kinds of building blocks under different pH and temperature conditions.

In this work, compound **1** represents an exception to the aforementioned examples. Compound **1** was synthesized with a mixture of $Na_2MoO_4\cdot 2H_2O$, $CuCl_2\cdot 2H_2O$,

Table 1. Comparison of the synthetic conditions of various compounds from the $\{MoO_x/P/TM/L\}$ system.

Compound[a]	Approx. pH	T [°C]	t [d]	Ref.
I. $[\{Ni(phen)\}_2PMo^{V}_3Mo^{VI}_9O_{40}]^{2-}$	3.8	160	7	[10a]
I. $[\{Cu(2,2'\text{-bpy})\}_{2.5}PMo^{V}_4Mo^{VI}_8O_{40}]^{2-}$	3.5	180	4	[10b]
I. $[\{Cu(4,4'\text{-bpy})\}_2HPMo_{11}CuO_{39}]^{2-}$	3.7	165	6	[10c]
I. $[\{Cu(2,2'\text{-bpy})\}PMo^{V}_2Mo^{VI}_{10}O_{40}]^{3-}$	3.8	165	4	[10d]
II. $[\{Mn(phen)_2(H_2O)_x\}_4\{Mn(P_4Mo_6(OH)_6O_{25})_2\}]^{2-}$	4.5	180[b]	6	[11a]
II. $[\{Cd(4,4'\text{-bpy})(H_2O)\}_2\{Cd(P_4Mo_6(OH)_6O_{25})_2\}]^{4-}$	5.0	170	5	[11b]
II. $[Na_3(P_4Mo_6(OH)_5O_{26})_2]^{11-}$	3.5	180	3	[11c]
II. $[Mn(P_4Mo_6O_{26}(OH)_5)_2]^{12-}$	4.0	250	2.5	[11d]
III. $[Co(en)_3]_2[P_2Mo_5O_{23}]$	3.0	160	6	[12a]
III. $[\{Cu(4,4'\text{-bpy})_2\}P_2Mo_5O_{23}]^{2-}$	4.5	160	6	[12b]
III. $[\{Ni(H_2O)_5\}\{Ni(4,4'\text{-Hbpy})(H_2O)_4\}P_2Mo_5O_{23}]^{-}$	3.0	160	6	[12c]

[a] I: Keggin-; II: $\{P_4Mo_6\}$-; III $\{P_2Mo_5\}$-building blocks. [b] The yield is improved at this reaction temperature.

phen, H_3PO_4, and $SrCl_2$ in a molar ratio of 1.00:0.30:0.30:4.80:0.50 in water at 160 °C for 4 d. The initial pH value was controlled in the range 3–4 with 1-M NaOH solution. If the reaction temperature was lower than 160 °C or the pH value was outside the 3–4 range, no crystals could be obtained. It is also interesting that when $SrCl_2$ was not introduced into the reaction mixture, another compound[17] was isolated under similar reaction conditions (T = 165 °C and pH = 3.5), which might be analogous to the polyoxoanion $[\{Ni(phen)\}_2PMo^{V}_3Mo^{VI}_9O_{40}]^{2-}$.[10a] Thus, it is supposed that the Sr^{2+} ions could be the necessary templates for the isolation of compound **1**.[18]

Structure Description

Single-crystal X-ray diffraction analysis revealed that **1** consists of an interesting basket-like $[Sr\subset P_6Mo_{18}O_{73}]^{10-}$ polyoxoanion decorated with four $\{Cu(phen)(H_2O)_x\}$ (x = 1 and 2) fragments (Figure 2) and charge balanced with one $\{Cu(phen)(H_2O)_3\}$ unit. In the polyoxoanion of **1** (Figure 3 and Figure S1), all Mo centers exhibit a six-coordinate environment with Mo–O bond lengths in the range 1.672(8)–2.454(6) Å and O–Mo–O bond angles varying from 83.4(3) to 173.7(3)°. The six P centers display tetrahedral coordination geometry. The P–O bond lengths range from 1.503(7) to 1.577(7) Å, whereas the O–P–O bond angles vary from 107.2(4) to 112.8(4)°. The basket-like polyoxoanion can be separated into two parts, that is, the "handle" $\{P_4Mo_4\}$ unit and the "basket body" $\{P_2Mo_{14}\}$ segment (Figure 2). The $\{P_4Mo_4\}$ unit consists of four $\{MoO_6\}$ octahedra and four $\{PO_4\}$ tetrahedra, which are corner-linked together to form the handle moiety. The $\{P_2Mo_{14}\}$ unit exhibits a tetravacant Dawson-type structural feature. In comparison to the Dawson-type isomers and their tetravacant species[5c] (Scheme 1), we conclude that the $\{P_2Mo_{14}\}$ building block in **1** is derived from the γ-Dawson anion. It is noteworthy that Dawson anions and a series of its lacunary derivatives have extensively acted as building blocks to constitute novel complexes with various functionalities.[1,2a,5] Nevertheless, only six kinds of lacunary Dawson-type derivatives have ever been observed (Scheme S1). In **1**, the γ-$\{P_2Mo_{14}\}$ unit represents a new lacunary Dawson-type species in POM chemistry. The "handle" ($\{P_4Mo_4\}$ unit) and the "basket body" ($\{P_2Mo_{14}\}$ unit) moieties are connected together through the edge- and/or corner-sharing modes (Figure 3 and Figure S2). The whole basket-shaped cluster possesses C_{2v} symmetry (Figure S2). In the central cavity of the polyoxoanion, a Sr^{2+} ion is fully encapsulated, and it exhibits a nine-coordinate environment with the bond lengths of Sr–O in the range 2.570(7)–2.754(6) Å (Figure 3 and Figure S3). It is interesting that the cavity size of the basket-

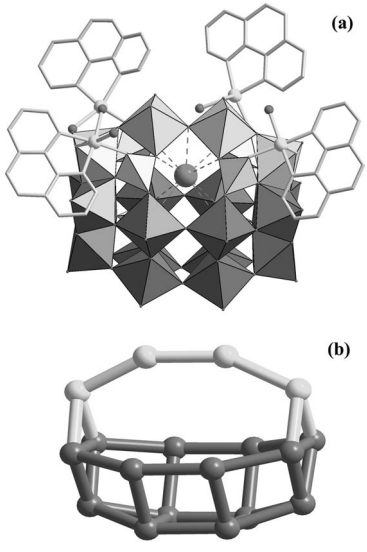

Figure 2. (a) Polyhedral and ball-and-stick representation of $[Sr\subset P_6Mo_{18}O_{73}]^{10-}$ decorated by four $\{Cu(phen)(H_2O)_x\}$ (x = 1 or 2) fragments in **1**. The isolated $\{Cu(phen)(H_2O)_3\}^{2+}$ unit is omitted for clarity. Octahedron, Mo; tetrahedron, P; large black ball, Sr; middle grey ball, Cu; Small black ball, O; grey line, phen ligand; (b) basket-like topology formed by 18 Mo atoms.

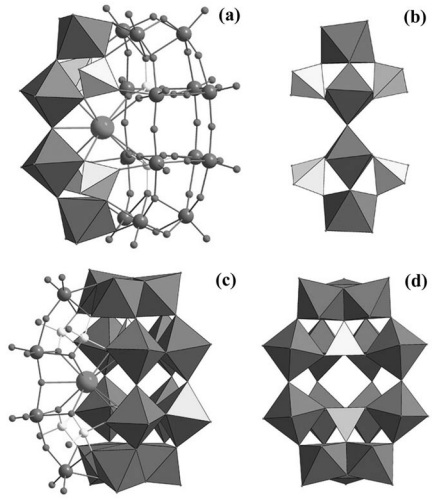

Figure 3. (a) Polyhedral and ball-and-stick representation of the basket-like $[Sr\subset P_6Mo_{18}O_{73}]^{10-}$ in **1**; (b) view of the "handle" $\{P_4Mo_4\}$ unit; (c) another view of the polyoxoanion of **1**; (d) view of the "basket body" $\{P_2Mo_{14}\}$ unit. Octahedron, Mo; tetrahedron, P; large black ball, Sr; middle black ball, Mo; small grey ball, P; small black ball, O.

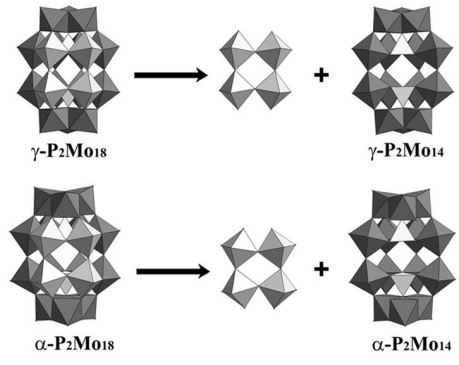

Scheme 1. Illustration of the comparison between α- and γ-Dawson-type polyoxoanions and their tetravacant derivatives.

like polyoxoanion seems to be more inclined to capture larger cations (Sr^{2+}) although both Sr^{2+} and Na^+ ions coexist in the reaction system with similar concentrations. Zhang et al. have also reported a similar $[P_6Mo_{18}O_{73}]^{11-}$ polyoxoanion encapsulating a K^+ ion.[13] The incorporation of these large cations may vice versa stabilize the whole cryptand polyoxoanion.[18]

In **1**, there are five independent $\{Cu(phen)(H_2O)_x\}$ (x = 1, 2, or 3) fragments. Four of them are coordinated directly to the surface of the polyoxoanion, whereas the fifth is isolated in the interspace of the crystal structure (Figure 4 and Figure S4). The Cu1 atom exhibits a five-coordinate environment with two O atoms from the polyoxoanion, two N atoms from the phen ligand, and one water ligand. The Cu2 atom possesses an octahedral coordination geometry with three O atoms from the polyoxoanion, two N atoms from the phen ligand, and one terminal water ligand. The Cu3 atom also displays octahedral coordination geometry with two O atoms from the polyoxoanion, two N atoms from the phen ligand, and two terminal water ligands. The $\{Cu(4)(phen)(H_2O)\}$ moiety is disordered in two positions (Figure S4). Both of the disordered parts exhibit a four-coordinate environment. The Cu5 atom has a five-coordinate environment, involving two N atoms from the phen ligand and three coordinated water molecules. The bond lengths of Cu–N and Cu–O are in the range 1.983(1)–2.122(2) and 1.912(2)–2.619(3) Å, respectively. It is noteworthy that two $\{Cu(2)(phen)(H_2O)\}$ units act as bridges to link two polyoxoanions into a dimeric cluster (Figure 4). In the packing arrangement, the adjacent $[\{Cu(phen)(H_2O)_2\}\{Cu(phen)(H_2O)\}_3\{Sr\subset P_6Mo_{18}O_{73}\}]^{2-}$ dimeric clusters are linked together by π–π interactions between adjacent phen groups to form a three-dimensional supramolecular framework (Figure S5). The isolated $\{Cu(phen)(H_2O)_3\}$ units are also connected with their adjacent coordinated analogues through π–π interactions between the phen groups. In the crystal structure, the average distance between two phen planes with π–π interactions is about 3.52 Å. The lattice water molecules should be extensively H-bonded with the surface oxygen atoms of the polyoxoanions. The typical H-bond lengths between them are as follows: OW1···O48 2.823 Å, OW2···O5 3.168 Å, OW3···O46 2.845 Å, and OW4···O22 3.454 Å.

In compound **1**, all P, Cu, and Sr centers exhibit +5, +2, and +2 oxidation states, respectively, on the basis of their coordination environments, bond lengths and angles, and the bond valence sum (BVS) calculation.[19] In addition, the black color of the crystal suggests that the Mo centers in compound **1** should be mixed valent. BVS calculation shows an average value of ca. 5.79 for all Mo centers (Table S3), which is close to the result of 14 Mo^{6+} and 4 Mo^{5+} in the polyoxoanion cluster. Considering the five $[Cu(phen)(H_2O)_x]^{2+}$ segments and no protonated oxygen atoms on the surface of the polyoxoanion, together with the BVS calculation results, the polyoxoanion formula can be expressed as $[Sr\subset P_6Mo^{V}_4Mo^{VI}_{14}O_{73}]^{10-}$. Furthermore, each Mo center on the γ-$\{P_2Mo_{14}\}$ unit contains just one Mo=O bond, whereas every Mo center on the "handle" $\{P_4Mo_4\}$ fragments possesses two Mo=O bonds, which suggests that the Mo centers on the γ-$\{P_2Mo_{14}\}$ unit are more easily reduced and that all four electrons could be delocalized only on the γ-$\{P_2Mo_{14}\}$ unit.[20a]

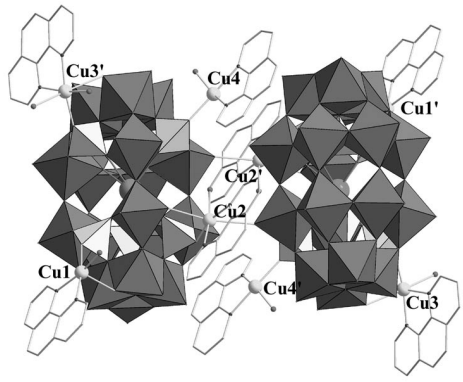

Figure 4. Polyhedral and ball-and-stick representation of the dimeric cluster of **1** and the coordination environments of the Cu centers. The isolated $\{Cu5(phen)(H_2O)_3\}$ unit is omitted for clarity. Octahedron, Mo; tetrahedron, P; large black ball, Sr; middle grey ball, Cu; small black ball, O; grey line, phen group.

XPS, UV/Vis, and IR Spectral Analyses

The oxidation states of Mo, Sr, and Cu in **1** are further confirmed by XPS measurements. The XPS spectrum of molybdenum indicates two overlapped peaks of Mo^{6+} and Mo^{5+} ions in the energy region of $Mo3d_{5/2}$ and $Mo3d_{3/2}$ (Figure 5a).[21a] The peaks of $Mo3d_{5/2}$ at 232.3 and 230.9 eV

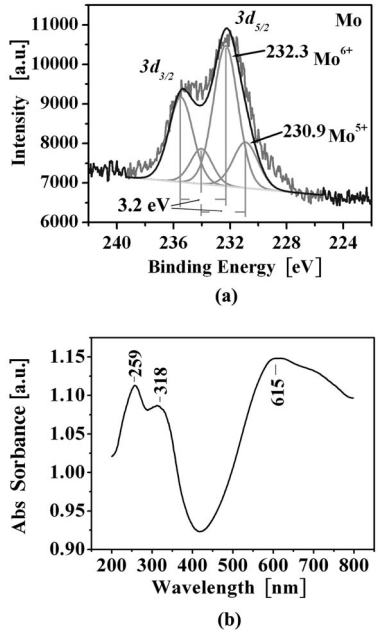

Figure 5. (a) The XPS spectrum of mixed-valent Mo in **1**. The fit line (black smooth line on the top) is produced by the decomposition of the overlapping peaks of Mo^{6+} and Mo^{5+} (middle and bottom grey lines) with a peak/area ratio of ca 3.5:1; (b) solid-state UV/Vis spectrum of **1**.

are attributable to the Mo^{6+} and Mo^{5+} ions, respectively.[21a] The best fit (top black line in Figure 5a) for the XPS spectrum of the mixed-valent Mo compound is produced by decomposition of the overlapping peaks of Mo^{6+} and Mo^{5+} with a peak/area ratio of ca. 3.5:1, which corresponds to the 14 Mo^{VI} and 4 Mo^{V} centers in compound **1**. This result is consistent with the BVS calculation and the charge-balance consideration. The XPS measurements were also carried out in the energy region of $Sr3d_{5/2}$ and $Cu2p_{3/2}$, respectively. The peaks at 133.2 eV and 932.4 eV are ascribed to Sr^{2+} and Cu^{2+} ions, respectively (Figure S6).[21b,21c]

The diffuse reflectance UV/Vis spectrum of compound **1** was also investigated with the solid-state sample in $BaSO_4$ pellet (Figure 5b). The two peaks at 259 and 318 nm are associated with two kinds of O–Mo LMCT bands,[20a] whereas the other strong wide band around 615 nm is due to overlap of several bands of the intervalence transition from Mo^{V} to Mo^{VI} by the Mo–O–Mo bond, the d–d transitions of Mo^{V} octahedra,[20a] and the Cu–$N_{(phen)}$ and Cu–$O_{(POM)}$ LMCT bands,[20b] which leads to the dark blue coloration of this compound.

In the IR spectrum of compound **1** (Figure S7), the characteristic peaks concerned with coordinated *o*-phenanthroline are at 1598(m), 1509(m), and 1430(s) cm^{-1}. Peaks at 1086(s) and 1025(w) cm^{-1} are assigned to the P–O vibrations and those at 923(s), 840(s), 769(s), and 711 cm^{-1} are attributed to the Mo=O and Mo–O–Mo vibrations of the polyoxoanion cluster.[20a]

Magnetic Properties

Solid-state variable-temperature magnetic susceptibility measurements were performed on the polycrystalline samples of **1** suspended in eicosane to prevent torquing. The DC magnetic susceptibility (χ_M) data were measured in the temperature range 1.8–300 K in a 1 T magnetic field and are plotted as $\chi_M T$ versus T in Figure 6. For **1**, the $\chi_M T$ product of 1.97 $cm^3 K mol^{-1}$ at 300 K decreases continuously to 1.92 $cm^3 K mol^{-1}$ at 1.8 K. The $\chi_M T$ value at room temperature is much lower than the spin-only value (g = 2.0) of 3.375 $cm^3 K mol^{-1}$ for five Cu^{2+} and four Mo^{5+} noninteracting ions (S = 1/2), but close to the value of 1.875 $cm^3 K mol^{-1}$ for five isolated Cu^{2+} ions. This result suggests that four delocalized electrons in each polyoxoanion cluster might be totally antiferromagnetically coupled, which has yet to be observed.[22] The $1/\chi_M$ versus T curve is consistent with the Curie–Weiss law with C = 1.98 $cm^3 K mol^{-1}$ and θ = –0.1 K, which indicates the presence of very weak antiferromagnetic interactions in the whole compound.

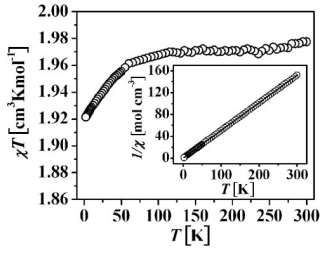

Figure 6. $\chi_M T$ vs. T curve of **1**; inset: $1/\chi_M$ vs. T curve. The solid line is the fitted result based the on Curie–Weiss law.

Thermogravimetric (TG) Analysis

The thermal behavior of compound **1** was investigated between 50 and 930 °C. The TG curve of this compound presents a three-step weight-loss process (Figure S8). The first step in the temperature range 80–300 °C corresponds to the loss of isolated and coordinated water molecules (calcd. weight loss 4.32%; found 4.43%). The second step occurs between 400 and 600 °C and corresponds to the loss of the *o*-phenanthroline ligands on copper centers (calcd. weight loss 19.65%; found 20.94%). The third step in the temperature range 760–930 °C is probably due to the evaporation of P_2O_5 (calcd. weight loss 18.57%; found 17.10%). The result of the TG analysis basically agrees with that of the structure determination.

Electrochemical and Electrocatalytic Properties

Although compound **1** was obtained from an aqueous system, it cannot be dissolved in water or a weak acidic aqueous solution. Therefore, its electrochemical behavior was investigated with a **1**-modified carbon paste electrode (**1**-CPE).[23] The cyclic voltammetric behavior for **1**-CPE in 1-M H_2SO_4 aqueous solution at different scan rates were recorded (Figure S9a) and they exhibit three reversible redox peaks in the potential range +800 to –100 mV, which is attributable to the $[Sr{\subset}P_6Mo_{18}O_{73}]^{10-}$ polyanions. At scan rates lower than 100 $mV s^{-1}$, the peak currents were proportional to the scan rate (Figure S9b), which indicates that the redox process of **1**-CPE is surface controlled. It is noteworthy that **1**-CPE possesses high stability. When the potential range is maintained at +800 to –100 mV, the peak currents almost remain unchanged over 300 cycles at a scan rate of 100 $mV s^{-1}$. After **1**-CPE was stored at room temperature for one month, the peak current decreased by only 3% and could be renewed by squeezing a little carbon paste out of the tube. The high stability of **1**-CPE could be ascribed to the organic–inorganic hybrid structural feature of **1** that stabilizes the polyoxoanion in the compound. Further, compound **1** is insoluble in the acidic aqueous media used in this experiment, which avoids the loss of the modifier during measurements. Thus, **1**-CPE could be an ideal electrode material to investigate electrocatalytic properties. Actually, **1**-CPE displays good electrocatalytic activity towards the reduction of hydrogen peroxide (Figure 7). At the **1**-CPE, with the addition of H_2O_2, all three reduction peak currents increased, whereas the corresponding oxidation peak currents dramatically decreased, which suggests that H_2O_2 was electrocatalytically reduced by all three reduced polyoxoanion species.[23,24] Furthermore, the cata-

lytic activities were enhanced with the increasing extent of the anion reduction. In contrast, the reduction of H_2O_2 at a bare electrode generally requires a large overpotential and no obvious response was observed at a bare CPE.

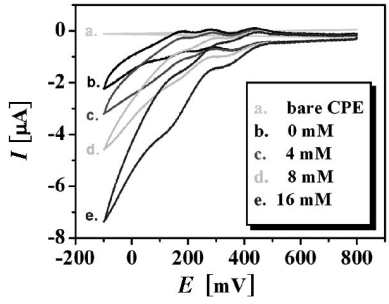

Figure 7. Cyclic voltammograms of **1**-CPE in H_2SO_4 (1 M) containing 0.0, 4.0, 8.0, and 16.0 mM H_2O_2 and a bare CPE in 5.0-mM H_2O_2 + 1-M H_2SO_4 solution. Potentials vs. SCE. Scan rate: 30 mV s^{-1}.

Conclusions

In this paper, we report organic–inorganic hybrid compound **1**, which exhibits a four-electron-reduced basket-like polyoxoanion modified with four $\{Cu(phen)(H_2O)_x\}$ (x = 1 and 2) fragments. Electrochemical analysis shows that **1**-CPE displays good electrocatalytic activity to reduce hydrogen peroxide. During the preparation of **1**, the use of Sr^{2+} ions led to the successful isolation of this new hybrid compound, which can serve as a basis for a new type of POM building block. Future efforts will be focused on the reactions between various functional organic–metal fragments and the basket-shaped polyoxoanion to obtain more $[Sr\subset P_6Mo_{18}O_{73}]$-based compounds. Furthermore, the templating effect of Sr^{2+} may also play an important role in the formation of $[Sr\subset P_6Mo_{18}O_{73}]^{10-}$; thus, other alkaline earth metal ions such as Ca^{2+} and Ba^{2+} will be introduced into this reaction system to check whether this templating effect could be reproduced.

Experimental Section

Materials: All chemicals purchased were of reagent grade and used without further purification.

Physical Methods: Elemental analyses (C, H, N) were performed with a Perkin–Elmer 2400 CHN elemental analyzer. Mo, Cu, P, and Sr were determined with a Leaman inductively coupled plasma (ICP) spectrometer. IR spectrum was recorded in the range 400–4000 cm^{-1} with an Alpha Centaurt FT/IR spectrophotometer with a pressed KBr pellet. Diffuse reflectance UV/Vis spectrum ($BaSO_4$ pellet) was obtained with a Varian Cary 500 UV/Vis NIR spectrometer. X-ray photoelectron spectrum (XPS) analyses were performed with a VG ESCALAB MK II spectrometer with a Mg-K_α (1253.6 eV) achromatic X-ray source. The vacuum inside the analysis chamber was maintained at 6.2×10^{-6} Pa during analysis. Magnetic susceptibility measurements were carried out with the use of a Quantum Design SQUID MPMS-XL susceptometer. DC measurements were conducted from 1.8 to 300 K by using a 1-T field and performed on finely ground polycrystalline samples. The magnetic data were corrected for the diamagnetic contribution calculated from Pascal's constants.[25] TG analysis was performed with a Perkin–Elmer TGA7 instrument in flowing N_2 with a heating rate of 10 °C min^{-1}. The electrochemical measurement was carried out on a CHI 660 electrochemical workstation at room temperature (25–30 °C).

1-Modified Carbon Paste Electrode (1-CPE): Graphite powder (1.0 g) and compound **1** (40 mg) were mixed and ground together with an agate mortar and pestle to achieve an even and dry mixture. Nujol (0.66 mL) was then added to the mixture and stirred with a glass rod. The homogenized mixture was used to pack glass tubes with a 3-mm inner diameter, and the surface was wiped with weighing paper. Electrical contact was established with a copper rod through the back of the electrode. Platinum gauze was used as the counter electrode and an SCE as the reference electrode.

Compound 1: A mixture of $Na_2MoO_4{\cdot}2H_2O$ (0.930 g), $CuCl_2{\cdot}2H_2O$ (0.204 g), phen (0.216 g), H_3PO_4 (0.838 mL, 85 wt.-%), and $SrCl_2$ (0.317 g) in a molar ratio of 1.00:0.30:0.30:4.80:0.50 was dissolved in H_2O (16 mL) and stirred at room temperature for 30 min. During this period, the pH value of the solution was adjusted to ca. 3.5 with a solution of NaOH (1 M). The final mixture was sealed in a 30-mL Teflon-lined stainless steel reactor and heated at 160 °C for 4 d. The dark-blue crystals were isolated and collected by filtration, washed thoroughly with distilled water, and dried at room temperature. Yield: 65% (based on Mo). $C_{60}H_{62}Cu_5Mo_{18}N_{10}O_{84}P_6Sr$ (4585.26): calcd. C 15.72, H 1.36, N 3.05, P 4.05, Cu 6.93, Mo 37.66, Sr 1.91; found C 15.79, H 1.42, N 3.11, P 3.99, Cu 7.01, Mo 37.69, Sr 1.87.

X-ray Crystallography: Single crystal of **1** with the size of $0.27\times0.25\times0.23$ mm was mounted on a glass fiber, and the data were collected with a Bruker SMART CCD diffractometer with graphite-monochromated Mo-K_α radiation (λ = 0.71073 Å). Semi-empirical absorption correction based on symmetry equivalent reflections was applied. A total of 41645 reflections were collected, of which 19453 reflections were unique [R(int) = 0.0516]. The structure was solved by direct methods and refined by the full-matrix least-squares method based on F^2. Structure solution, refinement, and generation of publication materials were performed with the use of the SHELXTL crystallographic software package.[26] During the refinement, the [Cu(4)(phen)(H_2O)] unit is disordered in two

Table 2. Crystal data and structure refinement for **1**.

Chemical formula	$C_{60}H_{62}Cu_5Mo_{18}N_{10}O_{84}P_6Sr$
Formula weight	4585.26
Crystal system	triclinic
Space group	$P\bar{1}$
a [Å]	13.778(3)
b [Å]	19.267(4)
c [Å]	24.168(5)
α [°]	110.64(3)
β [°]	90.31(3)
γ [°]	110.02(3)
V [Å^3]	5582.8(19)
Z	2
$D_{calcd.}$ [mg m^{-3}]	2.728
Absorption coefficient [mm^{-1}]	3.554
T [K]	293(2)
Reflections collected/unique	41645/19453 [R(int) = 0.0516]
Goodness of fit on F^2	1.022
R_1[a]	0.0497
wR_2[b]	0.1394

[a] $R_1 = \Sigma||F_o| - |F_C||/\Sigma|F_o|$. [b] $wR_2 = \Sigma[w(F_o^2 - F_c^2)^2]/\Sigma[w(F_o^2)^2]^{1/2}$.

positions with the site occupancies of 44 and 56%, respectively. All non-hydrogen atoms were refined with anisotropic parameters. The H atoms on the C atoms of phen were included in calculated positions with the use of a riding model and refined with fixed isotropic thermal parameters. The H atoms on water molecules were not included and just put into the final molecular formula. The largest residual peak (2.494 e$Å^{-3}$) is near the phen group but featureless, Q1···C46 0.583 Å. The deepest hole is –1.737 e$Å^{-3}$, which is close to the Mo8 atom. A summary of the crystal data is presented in Table 2. Atomic coordinates and isotropic displacement parameters for **1** are listed in Table S1, and selected bond lengths and angles are listed in Table S2. CCDC-642168 contains the supplementary crystallographic data for this paper. These data can be obtained free of charge from The Cambridge Crystallographic Data Centre via www.ccdc.cam.ac.uk/data_request/cif.

Supporting Information (see footnote on the first page of this article): Additional structural figures and packing arrangement views of **1**, additional XPS spectra, IR spectrum, TG curve, and CV analyses for compound **1**.

Acknowledgments

This work was supported by the National Natural Science Foundation of China (grant no. 20371014, 20671026, and 20701005) and Science Foundation for Young Teachers of Northeast Normal University (grant no. 20070302/20070312).

[1] a) P. Gouzerh, A. Proust, *Chem. Rev.* **1998**, *98*, 77–111; b) P. Gouzerh, R. Villanneau, R. Delmont, A. Proust, *Chem. Eur. J.* **2000**, *6*, 1184–1192; c) Special Issue on Polyoxometalates: C. L. Hill (Ed.), *Chem. Rev.* **1998**, *98*, 1–390; d) M. T. Pope, A. Müller (Eds.), *Polyoxometalate Chemistry: From Topology via Self-Assembly to Applications*, Kluwer, Dordrecht, The Netherlands, **2001**; e) T. Yamase, M. T. Pope (Eds.), *Polyoxometalate Chemistry for Nano-Composite Design*, Kluwer, Dordrecht, The Netherlands, **2002**; f) D. L. Long, E. Burkholder, L. Cronin, *Chem. Soc. Rev.* **2007**, *36*, 105–121; g) E. Coronado, C. Gimenez-Saiz, C. J. Gomez-Garcia, *Coord. Chem. Rev.* **2005**, *249*, 1776–1796.

[2] a) P. J. Hagrman, D. Hagrman, J. Zubieta, *Angew. Chem. Int. Ed.* **1999**, *38*, 2638–2684; b) E. Burkholder, V. Golub, C. J. O'Connor, J. Zubieta, *Inorg. Chem.* **2003**, *42*, 6729–6740; c) E. Burkholder, V. Golub, C. J. O'Connor, J. Zubieta, *Inorg. Chem.* **2004**, *43*, 7014–7029.

[3] a) S. Bareyt, S. Piligkos, B. Hasenknopf, P. Gouzerh, E. Lacôte, S. Thorimbert, M. Malacria, *Angew. Chem. Int. Ed.* **2003**, *42*, 3404–3406; b) B. J. S. Johnsn, R. C. Schroden, C. C. Zhu, A. Stein, *Inorg. Chem.* **2001**, *40*, 801–808.

[4] a) Z. Peng, *Angew. Chem. Int. Ed.* **2004**, *43*, 930–935; b) J. Kang, B. Xu, Z. Peng, X. Zhu, Y. Wei, D. R. Powell, *Angew. Chem. Int. Ed.* **2005**, *44*, 6902–6905.

[5] a) X. K. Fang, T. M. Anderson, C. L. Hill, *Angew. Chem. Int. Ed.* **2005**, *44*, 3540–3543; b) X. K. Fang, T. M. Anderson, Y. Hou, C. L. Hill, *Chem. Commun.* **2005**, 5044–5046; c) B. Godin, J. Vaissermann, P. Herson, L. Ruhlmann, M. Verdaguer, P. Gouzerh, *Chem. Commun.* **2005**, 5624–5626.

[6] a) X. L. Wang, C. Qin, E. B. Wang, Z. M. Su, Y. G. Li, L. Xu, *Angew. Chem. Int. Ed.* **2006**, *45*, 7411–7414; b) H. Y. An, E. B. Wang, D. R. Xiao, Y. G. Li, Z. M. Su, L. Xu, *Angew. Chem. Int. Ed.* **2006**, *45*, 904–907.

[7] a) C. Y. Sun, Y. G. Li, E. B. Wang, D. R. Xiao, H. Y. An, L. Xu, *Inorg. Chem.* **2007**, *46*, 1563–1574; b) J. Lu, E. H. Shen, M. Yuan, Y. G. Li, E. B. Wang, C. W. Hu, L. Xu, J. Peng, *Inorg. Chem.* **2003**, *42*, 6956–6958; c) Y. G. Li, G. De, M. Yuan, E. B. Wang, R. D. Huang, C. W. Hu, N. H. Hu, H. Q. Jia, *Dalton Trans.* **2003**, 331–334.

[8] a) S.-T. Zheng, D.-Q. Yuan, H.-P. Jia, J. Zhang, G.-Y. Yang, *Chem. Commun.*, DOI: 10.1039/b617191e; b) C.-M. Wang, S.-T. Zheng, G.-Y. Yang, *Inorg. Chem.* **2007**, *46*, 616–618.

[9] a) Y. Xu, J. Q. Xu, K. L. Zhang, Y. Zhang, X. Z. You, *Chem. Commun.* **2000**, 153–154; b) G. Y. Luan, Y. G. Li, S. T. Wang, E. B. Wang, Z. B. Han, C. W. Hu, N. H. Hu, H. Q. Jia, *Dalton Trans.* **2003**, 233–235; c) J. P. Wang, P. T. Ma, J. Y. Niu, *Inorg. Chem. Commun.* **2006**, *9*, 1049–1052; d) L. L. Fan, E. B. Wang, Y. G. Li, H. Y. An, D. R. Xiao, X. L. Wang, *J. Mol. Struct.*, DOI: 10.1016/j.molstruc.2006.11.059; e) A. X. Tian, Z. G. Han, J. Peng, B. X. Dong, J. Q. Sha, B. Li, *J. Mol. Struct.* **2007**, *832*, 117–123.

[10] a) M. Yuan, Y. G. Li, E. B. Wang, C. G. Tian, L. Wang, C. W. Hu, N. H. Hu, H. Q. Jia, *Inorg. Chem.* **2003**, *42*, 3670–3676; b) Y. P. Bai, Y. G. Li, E. B. Wang, X. L. Wang, Y. Lu, L. Xu, *J. Mol. Struct.* **2005**, *752*, 54–59; c) Y. Lu, Y. Xu, E. B. Wang, J. Lü, C. W. Hu, L. Xu, *Cryst. Growth Des.* **2005**, *5*, 257–260; d) H. Jin, Y. F. Qi, E. B. Wang, Y. G. Li, X. L. Wang, C. Qin, S. Chang, *Cryst. Growth Des.* **2006**, *6*, 2693–2698.

[11] a) M. Yuan, E. B. Wang, Y. Lu, Y. G. Li, C. W. Hu, N. H. Hu, H. Q. Jia, *J. Solid State Chem.* **2003**, *170*, 192–197; b) Y. Ma, Y. G. Li, E. B. Wang, Y. Lu, X. L. Wang, X. X. Xu, *J. Solid State Chem.* **2006**, *179*, 2367–2375; c) R. D. Huang, F. C. Liu, Y. G. Li, M. Yuan, E. B. Wang, G. De, C. W. Hu, N. H. Hu, H. Q. Jia, *Inorg. Chim. Acta* **2003**, *349*, 85–90; d) L. Xu, Y. Q. Sun, E. B. Wang, E. H. Shen, Z. R. Liu, C. W. Hu, Y. Xing, Y. H. Lin, H. Q. Jia, *New J. Chem.* **1999**, *23*, 1041–1044.

[12] a) Y. Ma, Y. Lu, E. B. Wang, X. X. Xu, Y. Q. Guo, X. L. Bai, L. Xu, *J. Mol. Struct.* **2006**, *784*, 18–23; b) Y. Lu, Y. G. Li, E. B. Wang, J. Lü, L. Xu, R. Clérac, *Eur. J. Inorg. Chem.* **2005**, *7*, 1239–1244; c) Y. Lu, J. Lü, E. B. Wang, Y. Q. Guo, X. X. Xu, L. Xu, *J. Mol. Struct.* **2005**, *740*, 159–163.

[13] X. M. Zhang, H. S. Wu, F. Q. Zhang, A. Prikhod'ko, S. Kuwata, P. Comba, *Chem. Commun.* **2004**, 2046–2047.

[14] C. Peloux, A. Dolbecq, P. Mialane, J. Marrot, E. Rivière, F. Sécheresse, *Angew. Chem. Int. Ed.* **2001**, *40*, 2455–2457.

[15] C. Peloux, P. Mialane, A. Dolbecq, J. Marrot, F. Sécheresse, *Angew. Chem. Int. Ed.* **2002**, *41*, 2808–2810.

[16] a) J. Gopalakrishnan, *Chem. Mater.* **1995**, *7*, 1265–1275; b) S. H. Feng, R. R. Xu, *Acc. Chem. Res.* **2001**, *34*, 239–247; c) L. M. Zheng, T. Whitfield, X. Wang, A. J. Jacobson, *Angew. Chem. Int. Ed.* **2000**, *39*, 4528–4531; d) P. R. Hagrman, R. L. LaDuca, H.-J. Koo, R. Rarig, R. C. Haushalter, M.-H. Whangbo, J. Zubieta, *Inorg. Chem.* **2000**, *39*, 4311–4317.

[17] The crystal data of the unpublished compound cannot be successfully collected and solved owing to its poor crystal quality. The initial cell is a = 14.72 Å, b = 22.12 Å, c = 25.13 Å, α = 89.98°, β = 98.61°, γ = 90.05°, V = 8115 $Å^3$. Elemental analysis: Mo:Cu:P ≈ 4:1:0.33. The primary results of the compound are similar to the reported compound in ref.[10a]

[18] D.-L. Long, H. Abbas, P. Kogerler, L. Cronin, *J. Am. Chem. Soc.* **2004**, *126*, 13880–13881.

[19] I. D. Brown, D. Altermatt, *Acta Crystallogr., Sect. B* **1985**, *41*, 244–247.

[20] a) M. T. Pope, *Heteropoly and Isopoly Oxometalates*, Springer, Berlin, **1983**, pp. 8, 109; b) B. DasGupta, C. Katz, T. Israel, M. Watson, L. Zompa, *Inorg. Chim. Acta* **1999**, *292*, 172–181.

[21] a) T. A. Patterson, J. C. Carver, D. E. Leyden, D. M. Hercules, *J. Phys. Chem.* **1976**, *80*, 1700–1708; b) M. Imamura, N. Matsubayashi, H. Shimada, *J. Phys. Chem. B* **2000**, *104*, 7348–7353; c) S. Gonzalez, M. Perez, M. Barrera, A. R. Gonzalez Elipe, R. M. Souto, *J. Phys. Chem. B* **1998**, *102*, 5483–5489.

[22] a) D. C. Duncan, C. L. Hill, *Inorg. Chem.* **1996**, *35*, 5828–5835; b) E. Dumas, C. Debiemme-Chouvy, S. C. Sevov, *J. Am. Chem. Soc.* **2002**, *124*, 908–909.

[23] a) X. L. Wang, Z. H. Kang, E. B. Wang, C. W. Hu, *J. Electroanal. Chem.* **2002**, *523*, 142–149; b) X. L. Wang, Z. H. Kang, E. B. Wang, C. W. Hu, *Mater. Lett.* **2002**, *56*, 393–396.
[24] D. Martel, A. Kuhn, *Electrochim. Acta* **2000**, *45*, 1829–1836.
[25] E. A. Boudreaux, L. N. Mulay (Eds.), *Theory and Applications of Molecular Paramagnetism*, John Wiley & Sons, New York, **1976**.
[26] a) G. M. Sheldrick, *SHELXL97: Program for Crystal Structure Refinement*, University of Göttingen, Germany, **1997**; b) G. M. Sheldrick, *SHELXS97: Program for Crystal Structure Solution*, University of Göttingen, Germany, **1997**.

Received: April 3, 2007
Published Online: October 31, 2007

